



HAL
open science

A pH- and Metal-Actuated Molecular Shuttle in Water

Amine Kriat, Simon Pascal, Brice Kauffmann, Yann Ferrand, David Bergé-Lefranc,
Didier Gignes, Olivier Siri, Anthony Kermagoret, David Bardelang

► **To cite this version:**

Amine Kriat, Simon Pascal, Brice Kauffmann, Yann Ferrand, David Bergé-Lefranc, et al.. A pH- and Metal-Actuated Molecular Shuttle in Water. *Chemistry - A European Journal*, 2023, 29 (33), pp.e202300633. <10.1002/chem.202300633>. <hal-04615234>

HAL Id: hal-04615234

<https://hal.science/hal-04615234v1>

Submitted on 18 Jun 2024

HAL is a multi-disciplinary open access archive for the deposit and dissemination of scientific research documents, whether they are published or not. The documents may come from teaching and research institutions in France or abroad, or from public or private research centers.

L'archive ouverte pluridisciplinaire HAL, est destinée au dépôt et à la diffusion de documents scientifiques de niveau recherche, publiés ou non, émanant des établissements d'enseignement et de recherche français ou étrangers, des laboratoires publics ou privés.



Distributed under a Creative Commons CC BY 4.0 - Attribution - International License

A pH- and Metal-Actuated Molecular Shuttle in Water

Amine Kriat,^[a] Simon Pascal,^[b] Brice Kauffmann,^[c] Yann Ferrand,^[d] David Bergé-Lefranc,^[a] Didier Gimes,^[a] Olivier Siri,^[b] Anthony Kermagoret,^{*,[a]} and David Bardelang^{*,[a]}

Abstract: The structure of the Viologen-Phenylene-Imidazole (VPI) guest, previously shown to be bound by cucurbit[7]uril (CB[7]) with binding modes depending on pH and silver ions, has been extended by adding hydrophobic groups on the two extremities of VPI before investigations of CB[7] binding by NMR, ITC, X-ray diffraction, UV-vis and fluorescence spectroscopies. With an imidazole station extended by a naphthalene group (VPI-N), binding modes of CB[7] are similar to those previously observed. However, with the

viologen extended by a tolyl group (T-VPI), CB[7] preferentially sits on station T, shuttling between the T and P stations at acid pH or after Ag⁺ addition. The CB[7]·T-VPI complex thus behaves as a metal-actuated thermodynamic *stop-and-go* molecular shuttle featured by fast and autonomous ring translocation between two stations and a continuum for fractional station occupancy solely and easily controlled by Ag⁺ concentration.

Introduction

Since the discovery of molecular shuttles by Stoddart and coworkers in the early 1990s,^[1] there have been many reports^[2] describing for example restricted ring shuttling,^[3] modulation of shuttling speed^[4] or tuning of station occupancy.^[5] In this field, one could distinguish those for which ring shuttling is reversibly actuated by an external stimulus, in a switch-like manner,^[6] from those, often “rapid” for which ring shuttling occurs autonomously between two degenerate or near degenerate stations. However, few have been described, to the best of our knowledge, enabling to control the entry in the shuttle mode (*stop-and-go* molecular shuttles),^[7] and the majority of molecular shuttles have been studied in organic solvents. The discovery of cucurbituril macrocycles^[8] and especially CB[7] in 2000 (Figure 1)^[9] featured by relatively high affinities for guest

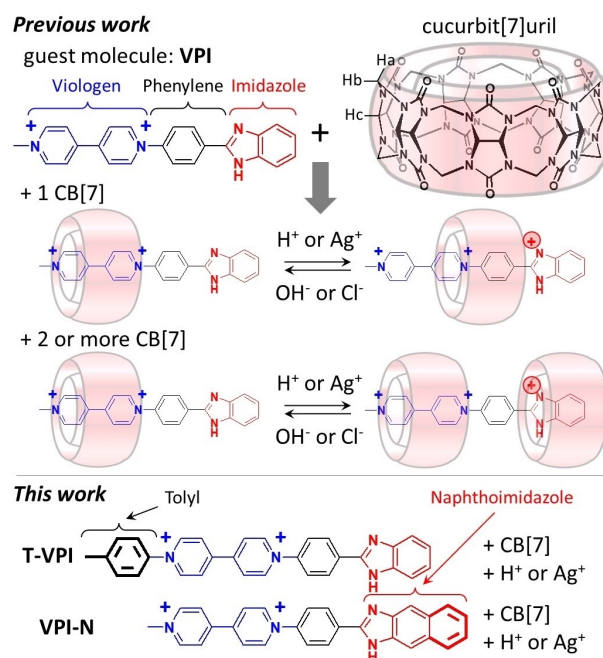


Figure 1. Molecular structures of VPI and CB[7] and main binding modes upon addition of H⁺ or Ag⁺. In this work, we extended the hydrophobic part of the guest on the viologen side by a tolyl group (T) or on the imidazole side by a naphthalene (N) and studied how this impacted CB[7] binding.

molecules^[10] enabled to prepare several molecular switches^[11] and shuttles^[12] in water. Yet and again, very few reports are available about cucurbituril based molecular shuttles in water. Kaifer and coworkers, the first, shown in 2006^[13] that a “fixed” CB[7] could reversibly enter a fast shuttling mode by acidification of a viologen dicarboxylate guest molecule, followed by similar results with a more rigid pseudo-rotaxane.^[14] In 2016, Ma and coworkers reported a pH gated CB[7] shuttle with tunable room-temperature phosphorescence.^[15] Recently,

[a] A. Kriat, Prof. D. Bergé-Lefranc, Dr. D. Gimes, Dr. A. Kermagoret, Dr. D. Bardelang
Aix Marseille Univ, CNRS, ICR, AMUtech, Marseille (France)
E-mail: anthony.kermagoret@univ-amu.fr
david.bardelang@univ-amu.fr
Homepage: <https://supra-mars.univ-amu.fr/>

[b] Dr. S. Pascal, Dr. O. Siri
Aix Marseille Univ, CNRS, CINAM, AMUtech, Marseille (France)

[c] Dr. B. Kauffmann
Univ. Bordeaux, CNRS, INSERM
Institut Européen de Chimie et Biologie (UAR3033/US001)
2 rue Escarpit, 33600 Pessac (France)

[d] Dr. Y. Ferrand
CNRS, Bordeaux Institut National Polytechnique, CBMN (UMR 5248)
Université de Bordeaux,
Institut Européen de Chimie et Biologie
33600 Pessac (France)

Supporting information for this article is available on the WWW under <https://doi.org/10.1002/chem.202300633>

© 2023 The Authors. Chemistry - A European Journal published by Wiley-VCH GmbH. This is an open access article under the terms of the Creative Commons Attribution License, which permits use, distribution and reproduction in any medium, provided the original work is properly cited.

McClenaghan, Parola, Basilio and coworkers reported a nice example of a CB[7] based molecular shuttle gated by light, pH and temperature.^[16] Beside the light-gated system mentioned above raising or lowering a kinetic barrier to exit or enter the shuttling mode, the other examples are based on one (or two) particular station(s) that is (are) rendered much less attractive for the host by a relevant stimulus thereby blocking the ring on another station. Strangely, there is no molecular shuttle in water sensitive to a stimulus improving ring binding on a disfavored station *enough* to reach the affinity of the first station (entry in autonomous shuttling), but *not enough* to trigger full ring translocation (quantitative single shuttling as in a switch).

Recently, we reported the pH-responsive viologen derivative VPI because of the three different stations CB[7] can dock on (Figure 1).^[17] While CB[8] formed a host-guest 2:2 complex with this guest,^[18] and CB[10], a host-guest 2:3 complex,^[19] results were very different with CB[7]. At one equivalent of host, with H⁺ or Ag⁺ cations, CB[7] quantitatively moved from station V to station P affording a pH- or metal-triggered ring translocation switch in water.^[17,20] Fostered by these findings, we wondered how structural extensions by hydrophobic fragments would impact CB[7] binding considering that the action of chemical stimuli (H⁺ or Ag⁺) was expected to modulate the outcome. We thus prepared two new compounds, extended on the imidazole side by a naphthyl group (VPI-N) and on the viologen side by a tolyl group (T-VPI) before investigating their interactions with CB[7] and the impact of pH and AgNO₃ on the binding modes. Finally, we found that H⁺ or Ag⁺ cations could enable the ring of a new host-guest complex to enter a fast autonomous shuttling mode by improving binding on a

previously disfavored station resulting in a new kind of thermodynamic molecular shuttle in water.

Results and Discussion

Synthesis

The synthesis of VPI-N is largely inspired from that used for VPI,^[20] and the preparation of T-VPI relies on well-known Zincke chemistry. Details of these syntheses and characterizations are described in Supporting Information.

CB[7] binding on VPI-N and T-VPI

The ¹H NMR spectrum of VPI-N in D₂O (Figure 2a) is featured by chemical shifts of all aromatic resonances that are upfield shifted (7.1–8.8 ppm range) compared to analogous signals of VPI (7.3–9.4 ppm range)^[17] suggesting possible aggregation but the signals remaining sharp, we assigned this spectrum to the possible formation of a VPI-N dimer in solution at 1 mM.^[21] In the presence of 3 equiv. of TFA (trifluoroacetic acid, Figure 3a), resonances in the aromatic region shifted downfield (7.5–9.4 ppm range) matching with the range of chemical shifts observed for VPI or VPI-H⁺,^[17] each signal closely positioned with respect to those of analogous protons of VPI and thereby suggesting that VPI-N-H⁺ is present as a monomer in solution. As for VPI, when one equiv. of CB[7] was added in a solution of VPI-N, signals corresponding to protons H₃ and H₄ are shifted upfield by 1.0 ppm (Figure 2b) in line with viologen

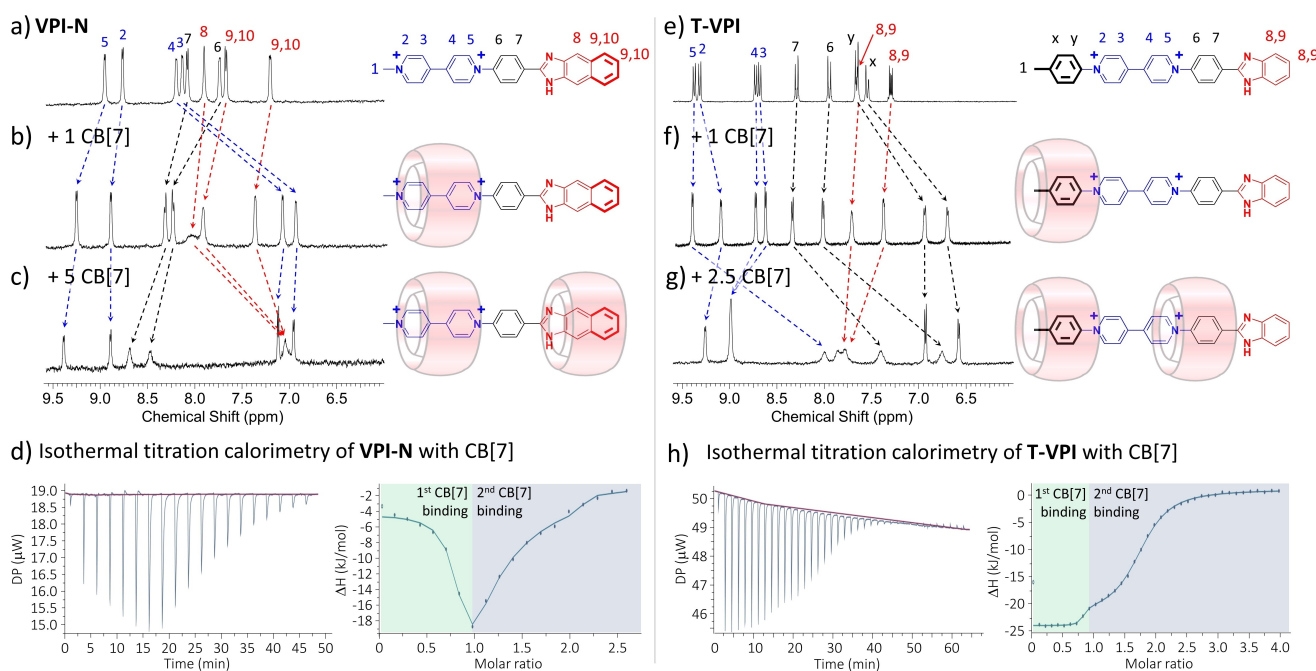


Figure 2. Aromatic part of 500 MHz ¹H NMR spectra of VPI-N (a) alone, (b) with 1 equiv. of CB[7] and (c) with 5 equiv. of CB[7] at 299 ± 1 K. Microcalorimetric titration (d) of VPI-N with CB[7] in line with two binding events (see text). Aromatic part of 500 MHz ¹H NMR spectra of T-VPI (e) alone, (f) with 1 equiv. of CB[7] and (g) with 2.5 equiv. of CB[7] at 299 ± 1 K. Microcalorimetric titration (h) of T-VPI with CB[7] in line with two binding events (see text).

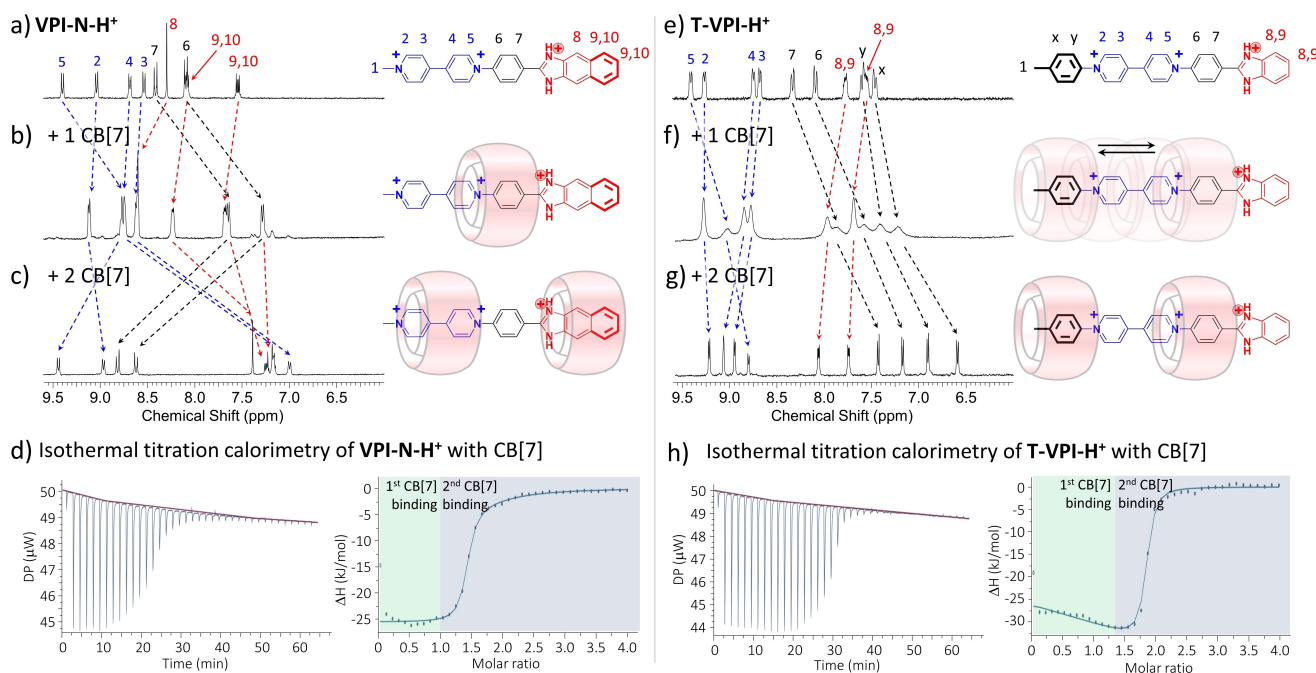


Figure 3. Aromatic part of ¹H NMR spectra of VPI-N-H⁺ (a) alone, (b) with 1 equiv. of CB[7] and (c) with 5 equiv. of CB[7] at 300 K. Microcalorimetric titration (d) of VPI-N-H⁺ with CB[7] in line with two binding events (see text). Aromatic part of ¹H NMR spectra of T-VPI-H⁺ (e) alone, (f) with 1 equiv. of CB[7] and (g) with 2 equiv. of CB[7] at 300 K. Microcalorimetric titration (h) of T-VPI-H⁺ with CB[7] in line with two binding events (see text).

complexation.^[20] However and contrary to the situation with VPI,^[17,20] a second binding is possible, on station N (Figure 2c) but requires an excess of CB[7]. In parallel of NMR studies, we investigated CB[7] binding by isothermal titration calorimetry (ITC) and observed an unusual V-shape thermogram for the titration of VPI-N with CB[7] (Figure 2d). Indeed, the ΔH values between 0 and 1 equiv. of host decreased before increasing after 1 equiv. of host. This behavior could be due to a dissociation of VPI-N dimers during an initial CB[7] binding, before a second complexation occurs with a larger enthalpic contribution after addition of more than 1 equiv. of host. Considering a 2:1 binding model, a good fit with experimental points was obtained affording stepwise binding constants $K_1 = 2.91 \times 10^5 \text{ M}^{-1}$ and $K_2 = 2.86 \times 10^3 \text{ M}^{-1}$. The K_1 value for binding of CB[7] on the viologen station is close to the one determined for VPI by ITC for the same binding ($K = 7.25 \times 10^5 \text{ M}^{-1}$).^[20] The relatively small value of K_2 for binding of the second CB[7] on station N is consistent with the need of several equivalents of host to saturate this station as monitored by NMR (Figure 2c). On the other hand, CB[7] behaved differently in the presence of T-VPI. Contrary to VPI or VPI-N, at 1 equiv. of host, CB[7] prefers sitting on station T of T-VPI, next to the viologen, as sometimes observed on viologen derivatives.^[12e,22] Indeed, 0.8 ppm upfield shifts of signals corresponding to protons H_x and H_y (Figure 2f) are assigned to the presence of CB[7] on station T. As for VPI-N though, a slight excess of host triggered a second binding of CB[7] but this time on station P as suggested by the upfield shifted signals of protons H₆ (1.1 ppm) and H₇ (0.8 ppm, Figure 2g). Titrations by ITC of solutions of CB[7] in solutions of T-VPI (Figure 2h) afforded thermograms consistent with a

stepwise binding of 2 CB[7] and binding constants $K_1 = 5.85 \times 10^7 \text{ M}^{-1}$ and $K_2 = 1.59 \times 10^5 \text{ M}^{-1}$. These values are close to those determined by competition NMR $K_1 = 3.2 \times 10^8 \text{ M}^{-1}$ (with respect to phenyl-trimethylammonium, Figure S31) and $K_2 = 2.9 \times 10^5 \text{ M}^{-1}$ (compared to 1-ethyl-3-methylimidazolium, Figure S32). These results are consistent with NMR data which suggested a quantitative binding of 1 equiv. of host on station T, and an about quantitative binding (requiring only a slight excess of host) on station P.

CB[7] binding on VPI-N and T-VPI at acid pH

As for VPI,^[17] when CB[7] was added on a solution of VPI-N-H⁺, the CB[7] host sited on station P (Figure 3b) as reflected by marked upfield shifts for signals of H₅ (Δδ = -0.6 ppm), H₆ (Δδ = -0.8 ppm), and H₇ (Δδ = -0.7 ppm). And as for VPI again, when 2 equiv. of host were used in the presence of TFA, there are 2 CB[7] sitting on the viologen and imidazole stations as shown by the diagnostic upfield shifts of signals of protons H₃ (Δδ = -1.5 ppm), H₄ (Δδ = -1.5 ppm), H₈ (Δδ = -0.8 ppm), H₉ (Δδ = -0.8 ppm), and H₁₀ (Δδ = -0.25 ppm, Figure 3c). We next recorded ITC thermograms for the titration of CB[7] with VPI-N at acid pH which confirmed these results (Figure 3d). Simulations according to a 2:1 binding mode afforded a good match with experimental points and binding constants $K_1 = 4.85 \times 10^6 \text{ M}^{-1}$ and $K_2 = 2.10 \times 10^4 \text{ M}^{-1}$. This K_1 value, higher than the one recorded in water at neutral pH ($2.91 \times 10^5 \text{ M}^{-1}$) is consistent with ring translocation on station P (Figure 3b) and also with the one recorded previously for binding of CB[7] on station P of

VPI with Ag^+ ($6.45 \times 10^6 \text{ M}^{-1}$),^[20] or H^+ ($10.4 \times 10^6 \text{ M}^{-1}$).^[17] The K_2 value is also higher at acid pH ($2.10 \times 10^4 \text{ M}^{-1}$) than the one at neutral pH ($2.86 \times 10^3 \text{ M}^{-1}$) reflecting better binding on station **N** when the imidazole is protonated. A large range of metal ions have previously been tested with **VPI**.^[20] As we found that only Ag^+ was impacting NMR spectra, we focused on this cation with the new guest molecules. With this stimulus, the results are very similar to those obtained with TFA (see Supporting Information). Therefore, the extension of the benzimidazole into a naphthimidazole did not change much the way **CB[7]** binds **VPI-N**, H^+ and Ag^+ cations providing results consistent with those previously obtained with **VPI**.

We then tested the influence of pH and added TFA to solutions of **T-VPI** containing 1 or 2 equiv. of **CB[7]**. With one host molecule, the ¹H NMR spectrum is featured by broad peaks (Figure 3f), the lack of resonance in the region corresponding to the signals of the phenylene possibly indicating that their position has been shifted upfield (other resonances at down field correspond to signals of viologen protons). The absence of sharp peaks also suggested that **CB[7]** could shuttle between at least 2 stations. Station **T** being largely preferred at neutral pH and station **P** being one of possible stations at acid pH (as for **VPI**), we hypothesized a shuttling of **CB[7]** between the **T** and **P** stations caused by protonation of the imidazole group of **T-VPI**. This is in line with previous reports on structurally similar guest compounds for **CB[7]**.^[17] With two **CB[7]** in an acidic solution of **T-VPI**, the ¹H NMR spectrum (Figure 3g) showed sharp peaks in line with tolyl and phenylene complexation, thereby supporting the previous hypothesis.

Indeed, upfield shifts of 0.8 and 1.1 ppm for signals of H_6 and H_7 , respectively (station **P**), and of 0.7 and 0.9 ppm for signals of H_x and H_y , respectively (station **T**), are in line with 2 **CB[7]** hosts firmly sitting on stations **T** and **P**. This shows that once protonated, **T-VPI-H⁺** has a clear preference to host **CB[7]** molecules on the stations **T** and **P** with a similar affinity. As previously done, we performed ITC titrations, this time of **CB[7]** in solutions of **T-VPI** at acid pH and recorded thermograms in line with double host binding. Simulations according to a 2:1 binding mode afforded a good fit with experimental points and similar binding constants $K_1 = 4.54 \times 10^6 \text{ M}^{-1}$ and $K_2 = 3.16 \times 10^6 \text{ M}^{-1}$, supporting the proposed shuttling of **CB[7]** between two stations of **T-VPI-H⁺**. Results obtained by ITC are summarized in Table 1.

As for **VPI-N**, the addition of AgNO_3 instead of TFA in solutions of **T-VPI** with **CB[7]** showed pretty similar ¹H NMR spectra leading to similar conclusions (see Supporting Informa-

tion). Therefore, adding another (tolyl) binding site on the viologen resulted in different **CB[7]** binding modes, the first **CB[7]** residing on station **T**, the second on station **P** showcasing a shifting in **CB[7]** docking from stations **V+I** (for **VPI**) to stations **T+P** (for **T-VPI**). The matching of affinities between stations **T** and **P** (after guest protonation) afforded a new molecular shuttle with fast autonomous ring translocation in water due to the near degeneracy of binding sites for **CB[7]** on **T-VPI-H⁺** and Brownian motion,^[23] temperature only marginally impacting host shuttling (288–348 K, Figure S43).

A short read at Table 1 shows large differences in enthalpic and entropic behaviour. For the **CB[7]·VPI-N** system, the first binding on station **V** is largely entropy-driven with an unusually small enthalpic value of -6.2 kJ mol^{-1} ($\Delta H_{\text{CB[7]·viologen}} = -16.7 \text{ kJ mol}^{-1}$,^[24] $\Delta H_{\text{CB[7]·VPI}} = -14.7 \text{ kJ mol}^{-1}$)^[20] which may originate from the (necessary) dissociation of the **VPI-N** dimer (energy penalty) before **CB[7]** can bind **VPI-N**. The second binding on uncharged station **N** is enthalpy-driven with a ΔH_2 value of $-45.6 \text{ kJ mol}^{-1}$ and is also featured by a large unfavourable entropy change. This trend is similar to the one observed for the binding of neutral guests, such as 3-diazabicyclo[2.2.2]oct-2-ene or cyclopentanone,^[25] by **CB[7]** and explained by the release of high-energy water molecules from the cavity of the host.^[26] This non-classical hydrophobic effect ($-\Delta \Delta S_2 > 0$) suggests that an entropic contribution, resulting from the release of water molecules from the naphthalene moiety to bulk water during complexation of station **N**, is significant.^[27,25]

For **VPI-N-H⁺**, this is the opposite. The first binding on station **P** is enthalpy-driven ($\Delta H_1 = -25.6 \text{ kJ mol}^{-1}$), but the second binding is entropy-driven ($-\Delta \Delta S_2 = -20.4 \text{ kJ mol}^{-1}$) with low ΔH_2 (-4.3 kJ mol^{-1}), perhaps due to the energetic penalty of relocating the first **CB[7]** on station **V** to allow the second **CB[7]** to dock on station **N** (or the opposite).

Without dimerization or host relocation for **T-VPI**, the two **CB[7]** bindings at neutral pH are both enthalpy-driven ($\Delta H_1 = -25.1 \text{ kJ mol}^{-1}$ and $\Delta H_2 = -21.6 \text{ kJ mol}^{-1}$) with a high total Gibbs enthalpy change ($\Delta G^\circ = -74 \text{ kJ mol}^{-1}$). The similarity of thermodynamic signatures for **CB[7]** binding on station **P** for (i) the **CB[7]·T-VPI** system and (ii) the **CB[7]·VPI-N-H⁺** system is consistent ($\sim 70\%$ ΔH° driven and $\sim 30\%$ ΔS° driven) in spite of the different protonated state of the guest. However, at acid pH, the two bindings (K_1 and K_2) are equal in magnitude but the first (binding and shuttling) is entropy-driven ($-\Delta \Delta S_1 = -26.8 \text{ kJ mol}^{-1}$) with a small value of $\Delta H_1 = -11.3 \text{ kJ mol}^{-1}$, while the second is largely enthalpy-driven ($\Delta H_2 =$

Table 1. Binding constants and thermodynamic parameters obtained by Isothermal Titration Calorimetry in water.^[a]

Species	K_1/M^{-1}	$\Delta H_1/\text{kJ mol}^{-1}$	$-\Delta \Delta S_1/\text{kJ mol}^{-1}$	K_2/M^{-1}	$\Delta H_2/\text{kJ mol}^{-1}$	$-\Delta \Delta S_2/\text{kJ mol}^{-1}$
CB[7]·VPI-N	$2.91 (\pm 0.61) \times 10^5$	$-6.2 (\pm 0.6)$	$-24.9 (\pm 1.1)$	$2.86 (\pm 0.21) \times 10^3$	$-45.6 (\pm 5.1)$	$+25.9 (\pm 5.3)$
CB[7]·T-VPI	$5.85 (\pm 0.14) \times 10^7$	$-25.1 (\pm 0.1)$	$-19.2 (\pm 0.2)$	$1.59 (\pm 0.09) \times 10^5$	$-21.6 (\pm 0.1)$	$-8.1 (\pm 0.2)$
CB[7]·VPI-N (acid pH)	$4.86 (\pm 0.10) \times 10^6$	$-25.6 (\pm 0.2)$	$-12.6 (\pm 0.3)$	$2.10 (\pm 0.15) \times 10^4$	$-4.3 (\pm 0.4)$	$-20.4 (\pm 0.6)$
CB[7]·T-VPI (acid pH)	$4.54 (\pm 0.21) \times 10^6$	$-11.3 (\pm 4.2)$	$-26.8 (\pm 4.3)$	$3.16 (\pm 0.06) \times 10^6$	$-54.3 (\pm 5.1)$	$+17.2 (\pm 5.2)$

[a] Binding model: two sets of sites.

$-54.3 \text{ kJ mol}^{-1}$) and entropy compensated ($-T\Delta S_2 = +17.2 \text{ kJ mol}^{-1}$). This may reflect some energy penalty at precisely locating a host which prefers shuttling (small ΔH_1 value), before the two CB[7] are fixed on stations T and P. Or, the CB[7] shuttling (non-specific interaction due to the energetic equivalence of binding sites T and P) could perturb guest solvation, enough to make the axle resembling an hydrophobic one since the thermodynamic signature ($\Delta H \ll 0$, $\Delta S > 0$) looks like the one for pure hydrophobic compounds.^[25] Unexpectedly, the thermodynamic behaviour is similar to the one observed for CB[7] binding on VPI-N even if the complexes involved are different.

A metal-actuated molecular shuttle. During our investigation of the CB[7]·T-VPI complex, and more specifically the molecular shuttle with excess H^+ , we wondered if we could progressively make the CB[7] ring shuttling from the T to the P station with Ag^+ . Recording ^1H NMR spectra of the 1:1 CB[7]·T-VPI complex with gradual addition of Ag^+ showed it is indeed the case (Figure 4) with progressive deshielding of signals corresponding to H_x and H_y protons suggesting that the T station is less and less occupied while at the same time, signals

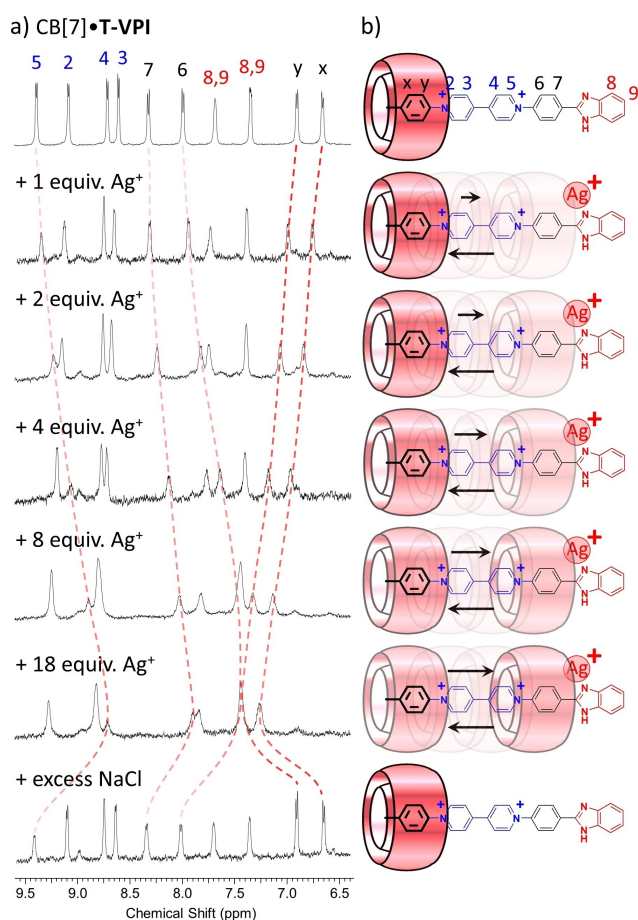


Figure 4. (a) Aromatic region of the 500 MHz ^1H NMR spectrum in D_2O (300 K) of the CB[7]·T-VPI complex with gradual addition of Ag^+ cations and (b) proposed gradual shuttling from no shuttle (top), CB[7] residing on station T up to rapid shuttling of the ring over the two T and P stations (bottom).

of protons 5, 6, and 7 progressively shifted upfield (CB[7] on station P). Variable-temperature (VT) NMR (Figure S56) did not allow to observe coalescence that would have enabled to determine activation energies and rates of exchange. However, the titration with increasing concentrations of Ag^+ unambiguously showed the autonomous and gradual, cation-triggered ring shuttling between the T and P stations.

X-ray diffraction

Single crystals of a host:guest 2:1 complex with silver could be grown from an aqueous solution of T-VPI with two CB[7] and excess AgNO_3 (^1H NMR spectrum, Figure 5a). The single-crystal structure (Figure 5b, CCDC number 2217466) confirmed the position of the first CB[7] on station T and that of the second CB[7] on station P. Beside the host:guest arrangement, one silver atom was found close to the imidazole function of T-VPI (Ag–N distance of 2.24 Å). The silver atom also interacts with two oxygen atoms of one carbonyl rim of the CB[7] ring docked on station P (Ag–O distances of 2.33 and 2.70 Å). The coordination sphere of silver is completed by one ordered water molecule (Ag–O distance of 2.42 Å). The structure of this

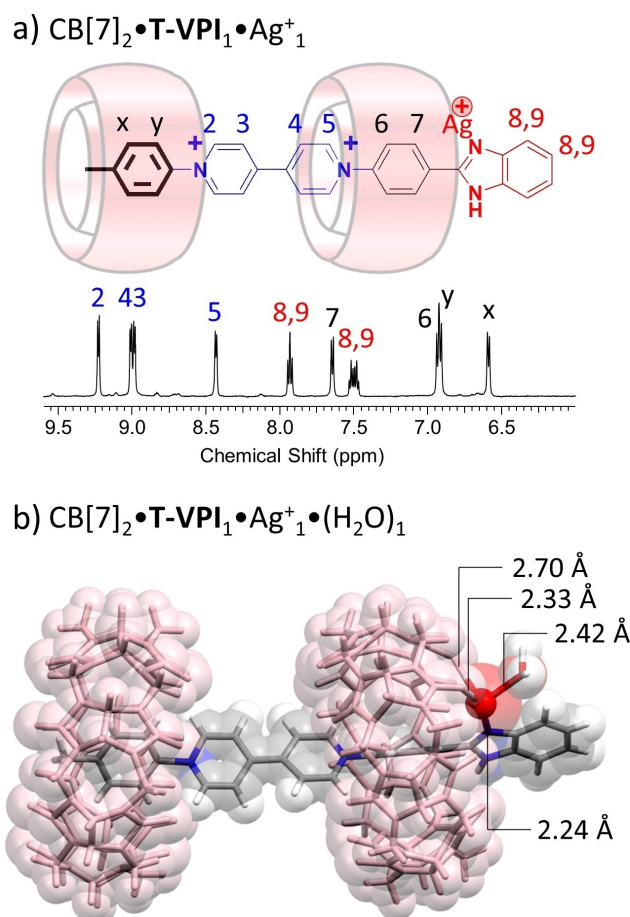


Figure 5. (a) Aromatic region of the 600 MHz ^1H NMR spectrum in D_2O (300 K) of the $\text{CB}[7]_2 \cdot \text{T-VPI} \cdot \text{Ag}^+$ complex and (b) X-ray structure of the same complex.

CB[7]₂·T-VPI·Ag⁺ complex confirms the previously postulated type of interactions for Ag⁺ ions with imidazole containing guest molecules and CB[7].^[20] Indeed, for VPI, CB[7] was postulated to be bound on station P with one silver ion coordinated by both, the guest by the imidazole nitrogen atom, and the host by two oxygen atoms of the closest carbonyl rim.^[20] Consistent with NMR results, the two CB[7] rings are found sitting on the T and P stations.

This type of double host binding implying *separated stations* (V+I or T+P) observed with VPI, VPI-N and T-VPI is most likely due to the impossibility for two CB[7] to sit simultaneously on adjacent stations.

UV-visible absorption and fluorescence spectroscopies

Contrary to VPI which is weakly or not fluorescent, VPI-T is emissive in solution which incited us to investigate the formation of these complexes by absorption and fluorescence spectroscopies (Figure 6 and Supporting Information). First, the comparison of the UV-vis spectra in water solution showed no important shift of absorption band upon addition of CB[7] for T-VPI and the corresponding protonated or coordinated species. Only a slight hypsochromic shift of the lower energy band was noticed for T-VPI in presence of 2 CB[7], presumably due to the presence of a macrocycle on the P station, interacting with the benzimidazole ring. Second, regarding the emission properties, T-VPI displays a weak fluorescence in the violet-blue range, peaking at 380 nm. The binding of a first CB[7] unit does not

shift the band, nevertheless, a second equivalent triggers a bathochromic shift of the emission band toward 398 nm. This observation is also consistent with the presence of a CB[7] at the proximity of the imidazole.

In the case of T-VPI·H⁺, a small redshift can be noticed upon addition of 1 equiv. of CB[7], which presumably reveals that the single host is shuttling between the T and P stations, in contrast with T-VPI that lacks such redshift. In the case of T-VPI·Ag⁺, the progressive bathochromic shift of the emission in presence of CB[7] also suggests that a comparable assumption can be formulated, but care has to be taken since the emissions are sensibly quenched by the coordination to silver, as can be noticed by the lower signal-to-noise ratio recorded.

Discussion

While binding of CB[7] on hydrophobic groups next to viologens (i.e. tolyl, phenylene) has been observed (in agreement with many previous reports),^[13,12e, 28, 14, 22] this trend remains difficult to explain. A possible reason may be that charge assisted N⁺C–H···O=C hydrogen bonds between the guest and the carbonyl crowns of the host may be stronger (more directional) when CB[7] is on the tolyl than when it is on the viologen for which such interactions would become more orthogonal so less stabilizing. At one equiv. of CB[7], H⁺ or Ag⁺ stimuli actuate CB[7] translocation from station V to station P (for VPI and VPI-N) or activate ring shuttling between stations T and P (for T-VPI). However, with 2 equiv. of host in solution, one CB[7] is always bound (either on station V or station T) before capture of the second CB[7], only at excess host, or when H⁺ or Ag⁺ cations are added, improving affinity of the second host for relevant stations. Even if representations of the CB[7] position along the guests are simplified for the sake of clarity throughout the paper, the atomic representation provided by the crystal structure affords more precise insights about CB[7] positioning. The unique interplay between Ag⁺ (or H⁺), CB[7] and VPI derivatives is probably, at least in part, responsible for the results observed, this kind of cooperative interaction being able to (i) actuate ring translocation, (ii) trigger shuttling between two stations or (iii) capture another macrocycle over a linear track. Figure 7 summarizes the supramolecular complexes discovered and the binding modes of CB[7] whether H⁺ or Ag⁺ ions are present or not. Hence, compared to previous results obtained with VPI, we found that hydrophobic extension by a naphthyl group on the imidazole did not change much the outcome regarding CB[7] binding with H⁺ or Ag⁺. The main difference being the possibility to complex the N station at high excess host, without H⁺ or Ag⁺. However, the introduction of a tolyl group on the other side (on the viologen) changed the site of the first binding to station T, created a shuttling motion in the presence of H⁺ or Ag⁺, and shifted the previously seen double binding from the V+I stations to the T+P stations. The serendipitous discovery of a metal-actuated molecular shuttle shows that other stimuli (here a metallic cation) can be used to enter the autonomous shuttle mode. This is possible because the asymmetric guest molecule

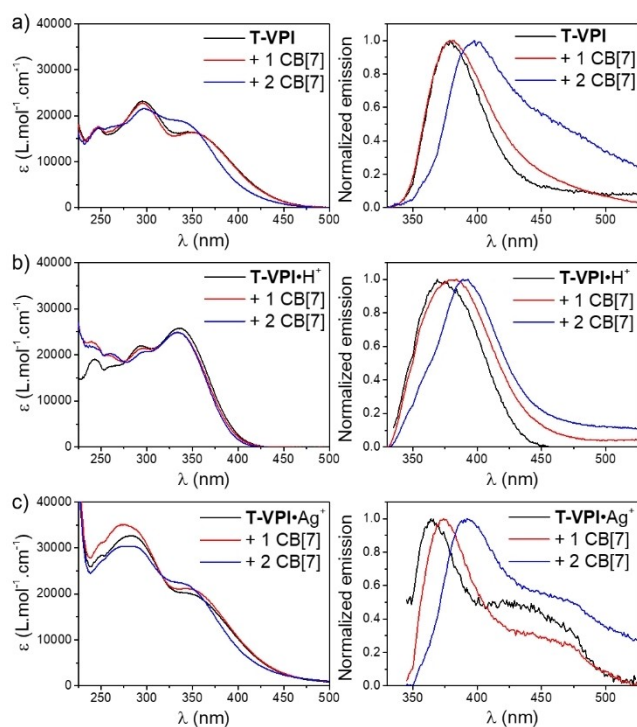


Figure 6. Electronic absorption (left) and fluorescence (right) spectra of T-VPI (10^{-5} M in H₂O) alone and with 1 or 2 CB[7] (a) at neutral pH, (b) at acid pH and (c) in the presence of 10 equiv. of Ag⁺ ions ($\lambda_{\text{exc}} = 290$ nm).

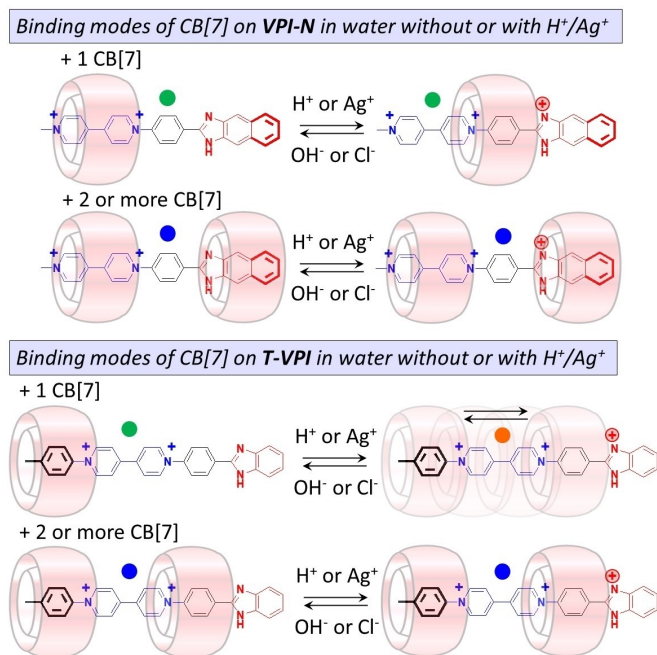


Figure 7. New supramolecular complexes obtained with VPI-N and with T-VPI in the presence of CB[7], without (left column) and with (right column) H⁺ or Ag⁺ stimuli (●: 1:1 complexes, ●: 2:1 complexes, ●: molecular shuttle).

T-VPI possesses one tolyl favoured station for CB[7] and another station becoming about as attractive for CB[7] as the tolyl after addition of H⁺ (quantitative binding of H⁺) or Ag⁺ (equilibrated Ag⁺:imidazole:CB[7] binding). Interestingly, there is a continuum accessible in the “degree of shuttling” due to the lability of the Ag⁺⋯N(guest)⋯O₂(CB[7]) interaction. Indeed, one can continuously manipulate the degree of shuttling by the simple control of the quantity of Ag⁺ added from the “stop state” to the about equally populated “autonomous shuttling state” with all intermediate situations.

Conclusions

In conclusion, we have explored how hydrophobic extensions on either end of a viologen-phenylene-imidazole (VPI) guest molecule impact CB[7] binding. Replacement of the initial benzimidazole unit by a naphthimidazole part (VPI-N) resulted in similar binding behaviours for CB[7], the only noticeable difference is the possibility for a second binding on the newly formed N station at excess host concentration. However, introduction of a tolyl group on the viologen side (T-VPI) showed marked changes, CB[7] binding first on the tolyl group (station T) followed by binding of a second CB[7] on the phenylene (station P). At acid pH, ring translocation or ring capture is observed for VPI-N (as for VPI) but for T-VPI, shuttling or second binding promotion is observed. For the three guest molecules, the addition of Ag⁺ ions led to the same complexation modes with CB[7] as with H⁺, but required excess metal

ion where H⁺ could be used stoichiometrically. Beside NMR enabling to propose binding modes of CB[7], ITC allowed to quantify the affinity of the hosts for precise stations of the guests confirming double host binding and strongly supporting the proposed shuttling of one CB[7] on protonated T-VPI. Finally, the single-crystal structure of the CB[7]₂·T-VPI·Ag⁺ complex allowed to confirm the binding mode of silver, linking simultaneously the host and the guest to stabilize a CB[7] on the best station.

Experimental Section

General: Chemicals and solvents were purchased from commercial sources (Aldrich, Acros, ABCR or TCI) and used without further purification. CB[7] was prepared according to a previous paper^[29] with extra caution regarding possible remaining acid traces. NMR measurements were recorded on Bruker AVL 300, 400, 500 or 600 spectrometers (see Supporting Information). When necessary for D₂O solutions, acetone was used as internal reference (2.22 ppm). CHN elemental analyses were performed using a Flash EA analyser, 1112 series Thermo Finnigan driven by the Eager 300 software (see Supporting Information). Isothermal Titration Calorimetry (ITC) experiments were performed on a Malvern MicroCal PEAQ-ITC titrating aqueous solutions of neutral CB[7] at 2 mM into aqueous solutions of guests (100 or 150 μM). For experiments at acid pH, solutions of CB[7] (2 mM) in aqueous HCl (0.5 mM) were titrated into solutions of guests (0.1 mM) in aqueous HCl (0.5 mM) carefully checking the pH was not decreasing below 2. Results were auto-analyzed using the Malvern MicroCal PEAQ-ITC Analysis Software. UV-visible absorption spectra were recorded in spectrophotometric grade water (ca. 10⁻⁵ M) on a VARIAN CARY 50 SCAN spectrophotometer at room temperature with a 300 nm/min scan rate. Emission spectra were measured using a Horiba-Jobin Yvon Fluorolog-3 spectrofluorimeter equipped with a three-slit double-grating excitation and a spectrograph emission monochromator with dispersions of 2.1 nm.mm⁻¹ (1200 grooves per mm). A 450 W xenon continuous wave lamp provided excitation. The luminescence of diluted solutions was detected at right angle using 10 mm quartz cuvettes.

X-ray diffraction

Deposition Number 2217466 contains the supplementary crystallographic data for this paper. These data are provided free of charge by the joint Cambridge Crystallographic Data Centre and Fachinformationszentrum Karlsruhe Access Structures service.

Synthesis: The syntheses of VPI-N and T-VPI are detailed in Supporting Information. All products were characterized by ¹H and ¹³C NMR (see Supporting Information, Figures S1 to S19). A counter anion metathesis was performed on VPI-N using a NO₃⁻ ion-exchange resin (see Supporting Information).

¹H NMR of VPI-N (500 MHz, D₂O, 3.3 · 10⁻⁴ M) δ 8.95 (d, J=5.3 Hz, 2H, H5), 8.76 (d, J=5.9 Hz, 2H, H2), 8.19 (d, J=5.4 Hz, 2H, H4), 8.13 (d, J=4.6 Hz, 2H, H3), 8.08 (d, J=8.0 Hz, 2H, H7), 7.90 (br s, 2H, H8), 7.73 (br s, 2H, H9 or H10), 7.67 (d, J=8.2 Hz, 2H, H6), 7.21 (dd, J=6.5, Hz J=3.0 Hz, 2H, H9 or H10), 4.31 (s, 3H, H1). Figure S7.

¹H NMR of T-VPI (300 MHz, D₂O) δ 9.38 (d, J=7.1 Hz, 2H, H5), 9.32 (d, J=7.1 Hz, 2H, H2), 8.74 (d, J=7.0 Hz, 2H, H4), 8.69 (d, J=7.0 Hz, 2H, H3), 8.31 (d, J=8.8 Hz, 2H, H7), 7.96 (d, J=8.8 Hz, 2H, H6), 7.68 (dd, J=5.8, 2.8 Hz, 4H, overlapped signals of H9 and H8), 7.57 (d,

$J=8.2$ Hz, 2H, **Hx**), 7.32 (dd, $J=6.1$, 3.2 Hz, 2H, **H9**), 2.47 (s, 3H, **H1**). Figure S15.

NMR of VPI-N with CB[7]: 1:1 complex. A 1 mM solution of CB[7]·VPI-N was prepared by addition of 125 μL of a 4 mM solution of VPI-N in D_2O , 100 μL of 5 mM solution of CB[7] in D_2O and 275 μL of D_2O . ^1H NMR of CB[7]·VPI-N (300 MHz, D_2O , 1 mM) δ 9.38 (d, $J=6.4$ Hz, 2H, **H5**), 9.02 (d, $J=6.5$ Hz, 2H, **H2**), 8.48 (d, $J=8.7$ Hz, 2H, **H7** or **H6**), 8.38 (d, $J=8.7$ Hz, 2H, **H7** or **H6**), 8.19 (s, 2H, **H8**), 8.06 (br s, 2H, **H9** or **H10**), 7.51 (br s, 2H, **H9** or **H10**), 7.21 (d, $J=6.4$ Hz, 2H, **H4**), 7.08 (d, $J=6.4$ Hz, 2H, **H3**), 5.73 (d, $J=15.4$ Hz, 14H, CB[7]), 5.54 (s, 14H, CB[7]), 4.25 (d, $J=15.5$ Hz, 14H, CB[7]), 2.22 (acetone, ref). Figure S20.

2:1 complex: A 0.2 mM solution of CB[7]·VPI-N was prepared by addition of 25 μL of a 4 mM solution of VPI-N in D_2O , 20 μL of a 5 mM solution of CB[7] in D_2O and 455 μL of D_2O ; then were added successively 4, 16, 60 and 100 μL of a 5 mM solution of CB[7] in D_2O to prepare solutions presenting VPI-N/CB[7] ratios of 1/1.2, 1/2, 1/5 and 1/10, respectively (Figure S22). NMR of VPI-N + 5 equiv CB[7]: ^1H NMR (500 MHz, D_2O) δ 9.49 (d, $J=5.7$ Hz, 2H, **H5**), 8.99 (d, $J=5.7$ Hz, 2H, **H2**), 8.79 (br s, 2H, **H7** or **H6**), 8.57 (br s, 2H, **H7** or **H6**), 7.22 (d, $J=6.4$ Hz, 2H, **H4**), 7.14 (br m, 6H, 2H, overlapped signals of **H8**, **H9** and **H10**), 7.06 (d, $J=5.7$ Hz, 2H, **H3**), 5.90–5.60 (m, 75H, CB[7]), 5.60–5.36 (m, 74H, CB[7]), 4.34–4.03 (m, 74H, CB[7]). Figure S23.

NMR of T-VPI with CB[7]: 1:1 complex. A 0.5 mM solution of CB[7]·T-VPI was prepared by addition of 125 μL of a 2 mM solution of T-VPI in D_2O ($2.5 \cdot 10^{-7}$ mol), 50 μL of 5 mM solution of CB[7] in D_2O ($2.5 \cdot 10^{-7}$ mol) and 325 μL of D_2O . ^1H NMR of CB[7]·T-VPI (500 MHz, D_2O , 0.5 mM) δ 9.49 (d, $J=6.4$ Hz, 2H, **H5**), 9.15 (d, $J=6.4$ Hz, 2H, **H2**), 8.79 (d, $J=4.7$ Hz, 2H, **H4**), 8.68 (d, $J=6.2$ Hz, 2H, **H3**), 8.43 (d, $J=8.4$ Hz, 2H, **H7**), 8.10 (d, $J=8.4$ Hz, 2H, **H6**), 7.78 (br s, 2H, **H8** or **H9**), 7.44 (dd, $J=5.9$, 3.1 Hz, 2H, **H8** or **H9**), 6.99 (d, $J=8.0$ Hz, 2H, **Hy**), 6.75 (d, $J=8.0$ Hz, 2H, **Hx**), 5.80 (two d, $J=15.4$ Hz, 14H, CB[7]), 5.50 (s, 14H, CB[7]), 4.21 (app dd, $J=15.4$, 9.2 Hz, 14H, CB[7]), 2.22 (acetone, ref), 2.09 (br s, 3H, **H1**). Figure S25.

2:1 complex: A 0.2 mM solution of CB[7]₂·T-VPI was prepared by addition of 50 μL of a 2 mM solution of T-VPI in D_2O (10^{-7} mol), 50 μL of a 5 mM solution of CB[7] ($2.5 \cdot 10^{-7}$ mol) in D_2O and 400 μL of D_2O . ^1H NMR of CB[7]₂·T-VPI (500 MHz, D_2O , 0.2 M, 298 K) δ 9.34 (d, $J=6.0$ Hz, 2H, **H2**), 9.06 (br m, 4H, **H3** and **H4**), 8.08 (br s, 2H, **H5**), 7.89 (br m, 4H, **H8** and **H9**), 7.47 (br s, 2H, **H7**), 7.01 (d, $J=8.2$ Hz, 2H, **Hy**), 6.83 (br s, 2H, **H6**), 6.65 (d, $J=8.0$ Hz, 2H, **Hx**), 5.78 (m, 32H, CB[7]), 5.53 (m, 33H, CB[7]), 4.22 (app t, $J=15.4$ Hz, 36H, CB[7]), 2.22 (acetone, ref), 2.02 (br s, 3H, **H1**). Figure S28.

NMR of VPI-N-H⁺ with CB[7]: VPI-N-H⁺. A solution of TFA–D (12.5 mM, 120 μL , $1.5 \cdot 10^{-6}$ mol) was added to a 1 mM solution of VPI-N in D_2O (500 μL , $0.5 \cdot 10^{-6}$ mol), leading to a pale-yellow solution. ^1H NMR of VPI-N-H⁺ (300 MHz, D_2O , 1 mM) δ 9.40 (d, $J=7.1$ Hz, 2H, **H5**), 9.04 (d, $J=6.9$ Hz, 2H, **H2**), 8.69 (d, $J=7.0$ Hz, 2H, **H4**), 8.54 (d, $J=6.9$ Hz, 2H, **H3**), 8.42 (d, $J=8.9$ Hz, 2H, **H7**), 8.30 (s, 2H, **H8**), 8.14–8.05 (m, 4H, overlapped signals of **H6** and **H9**), 7.55 (dd, $J=6.5$, 3.3 Hz, 2H, **H10**), 4.48 (s, 3H, **H1**). Figure S18.

1:1 complex: A 1 mM solution of CB[7]·VPI-N-H⁺ was prepared by addition of 125 μL of a 4 mM solution of VPI-N ($5 \cdot 10^{-7}$ mol) in D_2O , 100 μL of a 5 mM solution of CB[7] ($5 \cdot 10^{-7}$ mol) in D_2O , 120 μL of a 12.5 mM solution of TFA in D_2O ($1.5 \cdot 10^{-6}$ mol) and 155 μL of D_2O . ^1H NMR of CB[7]·VPI-N-H⁺ (400 MHz, D_2O , 1 mM) δ 9.15 (d, $J=6.1$ Hz, 2H, **H2**), 8.80 (m, 4H, overlapped signals of **H4** and **H5**), 8.65 (m, 4H, overlapped signals of **H3** and **H8**), 8.26 (m, 2H, **H9** or **H10**), 7.70 (m, 4H, overlapped signals of **H7** and **H9** or **H10**), 7.32 (d, $J=8.2$ Hz, 2H, **H6**), 5.71 (dd, $J=23.2$, 15.5 Hz, 14H, CB[7]), 5.55 (s, 13H, CB[7]), 4.58 (s, **H1**), 4.26 (dd, $J=15.4$, 8.4 Hz, 13H, CB[7]), 2.22 (acetone, ref). Figure S33.

2:1 complex: A 1 mM solution of CB[7]₂·VPI-N-H⁺ was prepared by addition of 125 μL of a 4 mM solution of VPI-N ($5 \cdot 10^{-7}$ mol) in D_2O , 200 μL of a 5 mM solution of CB[7] (10^{-6} mol) in D_2O , 120 μL of a 12.5 mM solution of TFA in D_2O ($1.5 \cdot 10^{-6}$ mol) and 55 μL of D_2O . ^1H NMR of CB[7]₂·VPI-N-H⁺ (300 MHz, D_2O , 1 mM) δ 9.51 (d, $J=7.0$ Hz, 2H, **H5**), 9.04 (d, $J=6.7$ Hz, 2H, **H2**), 8.89 (d, $J=8.8$ Hz, 2H, **H7**), 8.69 (d, $J=8.8$ Hz, 2H, **H6**), 7.46 (s, 1H, **H8**), 7.32 (dd, $J=6.4$, 3.3 Hz, 2H, **H9** or **H10**), 7.29–7.20 (m, 4H, overlapped signals of **H4** and **H9** or **H10**), 7.07 (d, $J=6.5$ Hz, 2H, **H3**), 5.86–5.65 (m, 28H, CB[7]), 5.67 (s, 3H, **H1**), 5.56 (s, 14H, CB[7]), 5.45 (s, 14H, CB[7]), 4.27 (d, $J=15.4$ Hz, 14H, CB[7]), 4.17 (dd, $J=15.4$, 2.3 Hz, 14H, CB[7]), 2.22 (acetone, ref). Figure S36.

NMR of T-VPI-H⁺ with CB[7]: T-VPI-H⁺. 5 μL of 3.5% DCI solution ($5 \cdot 10^{-6}$ mol) were added to a 1 mM solution of T-VPI in D_2O (500 μL , $0.5 \cdot 10^{-6}$ mol), leading to a colorless solution. ^1H NMR of T-VPI-H⁺: (300 MHz, D_2O) δ 9.44 (d, $J=5.3$ Hz, 2H, **H5**), 9.30 (d, $J=5.1$ Hz, 2H, **H2**), 8.78 (d, $J=5.4$ Hz, 2H, **H4**), 8.72 (d, $J=5.5$ Hz, 2H, **H3**), 8.37 (d, $J=7.1$ Hz, 2H, **H7**), 8.13 (d, $J=7.3$ Hz, 2H, **H6**), 7.80 (m, 2H, **H8**), 7.66–7.54 (m, 4H, overlapped signals of **H6** and **Hy**), 7.50 (d, $J=8.0$ Hz, 2H, **Hx**), 2.40 (s, 3H, **H1**). Figure S19.

1:1 complex: A 1 mM solution of CB[7]·T-VPI-H⁺ was prepared by addition of 250 μL of a 2 mM solution of T-VPI ($5 \cdot 10^{-7}$ mol) in D_2O , 100 μL of a 5 mM solution of CB[7] ($5 \cdot 10^{-7}$ mol) in D_2O , 10 μL of a 200 mM solution of TFA in D_2O ($2 \cdot 10^{-6}$ mol) and 150 μL of D_2O . The solution was diluted to 0.1 mM. ^1H NMR of CB[7]·T-VPI-H⁺ (500 MHz, D_2O , 0.1 mM) δ 9.33 (br s, **H2**), 9.08 (br s, **H5**), 8.89 (br s, **H4**), 8.81 (br s, **H3**), 8.02 (br s, **H8** or **H9**), 7.91 (s, **H7**), 7.74 (br s, **H8** or **H9**), 7.62 (s, **H6**), 7.46 (br s, **Hy**), 7.29 (br s, **Hx**), 5.81–5.67 (m, CB[7]), 5.52 (two s, CB[7]), 4.24 (d, $J=15.4$ Hz, CB[7]), 2.36 (s, **H1**), 2.22 (acetone, ref). Figure S39.

2:1 complex: A 0.5 mM solution of CB[7]₂·T-VPI-H⁺ was prepared by addition of 125 μL of a 2 mM solution of T-VPI ($2.5 \cdot 10^{-7}$ mol) in D_2O , 100 μL of a 5 mM solution of CB[7] ($5 \cdot 10^{-7}$ mol) in D_2O , 12 μL of a 100 mM solution of TFA in D_2O ($1.2 \cdot 10^{-6}$ mol) and 270 μL of D_2O . ^1H NMR of CB[7]₂·T-VPI-H⁺ (400 MHz, D_2O , 298 K, 0.5 mM) δ 9.27 (d, $J=7.0$ Hz, 2H, **H2**), 9.12 (d, $J=6.7$ Hz, 2H, **H4**), 9.00 (d, $J=6.9$ Hz, 2H, **H3**), 8.86 (d, $J=7.0$ Hz, 2H, **H5**), 8.12 (dd, $J=6.2$, 3.2 Hz, 2H, **H8** or **H9**), 7.80 (dd, $J=6.2$, 3.2 Hz, 2H, **H8** or **H9**), 7.49 (d, $J=8.6$ Hz, 2H, **H7**), 7.23 (d, $J=8.6$ Hz, 2H, **H6**), 6.97 (d, $J=8.4$ Hz, 2H, **Hy**), 6.65 (d, $J=8.3$ Hz, 2H, **Hx**), 5.75 (app ddd, $J=22.9$, 15.4, 9.8 Hz, 28H, CB[7]), 5.65–5.43 (m, 28H, 28H, CB[7]), 4.24 (app ddd, $J=23.7$, 15.5, 10.6 Hz, 28H, 28H, CB[7]), 2.22 (acetone, ref), 2.02 (br s, 3H, **H1**). Figure S44.

NMR of VPI-N·Ag⁺ with CB[7]: 1:1:1 complex: a 0.5 mM solution of CB[7]·VPI-N·Ag⁺ was prepared by addition of 62.5 μL of a 4 mM solution of VPI-N ($2.5 \cdot 10^{-7}$ mol) in D_2O , 50 μL of a 5 mM solution of CB[7] ($2.5 \cdot 10^{-7}$ mol) in D_2O , 25 μL of a 200 mM solution of AgNO₃ in D_2O ($5 \cdot 10^{-6}$ mol) and 380 μL of D_2O . ^1H NMR of CB[7]·VPI-N·Ag⁺ (500 MHz, D_2O , 300 K, 0.5 mM) δ 9.15 (d, $J=6.0$ Hz, 2H, **H2**), 8.76 (m, overlapped signals of **H4** and **H3**), 8.51 (br s, 2H, **H8**), 8.45 (d, $J=5.8$ Hz, 2H, **H5**), 8.21 (br s, 2H, **H9** or **H10**), 7.86 (d, $J=8.0$ Hz, 2H, **H7**), 7.60 (br s, 2H, **H9** or **H10**), 7.06 (d, $J=7.7$ Hz, 2H, **H6**), 5.69 (app dd, $J=23.2$, 15.5 Hz, 14H, CB[7]), 5.53 (s, 14H, CB[7]), 4.58 (br s, **H1**), 4.24 (d, $J=15.5$ Hz, 14H, CB[7]), 2.22 (acetone, ref). Figure S48.

2:1:1 complex: To a 0.5 mM solution of CB[7]·VPI-N·Ag⁺ ($2.5 \cdot 10^{-7}$ mol) was added 50 μL of a 5 mM solution of CB[7] in D_2O ($2.5 \cdot 10^{-7}$ mol). ^1H NMR of CB[7]₂·VPI-N·Ag⁺ (500 MHz, D_2O , 300 K, 0.5 mM) δ 9.49 (d, $J=5.9$ Hz, 2H, **H5**), 9.03 (d, $J=5.5$ Hz, 2H, **H2**), 8.98 (d, $J=8.3$ Hz, 2H, **H7**), 8.57 (d, $J=8.1$ Hz, 2H, **H6**), 7.50 (d, $J=7.6$ Hz, 1H, **H9**), 7.42–7.29 (m, 3H, overlapped signals of **H8**, **H10** and **H9**), 7.24 (two d, $J=16.8$, 6.8 Hz, 3H, overlapped signals of **H10** and **H4**), 7.16 (br s, 1H, **H8**), 7.07 (d, $J=5.5$ Hz, 2H, **H3**), 5.73 (dd, $J=15.0$, 7.2 Hz, 28H, CB[7]), 5.56 (s, 14H, CB[7]), 5.46 (s, 14H, CB[7]),

4.27 (d, $J = 15.6$ Hz, 14H, CB[7]), 4.17 (dd, $J = 15.4$, 3.0 Hz, 14H, CB[7]), 2.22 (acetone, ref). Figure S52.

NMR of T-VPI·Ag⁺ with CB[7]: 1:1:1 complex: A 0.5 mM solution of CB[7]·T-VPI·Ag⁺ was prepared by addition of 125 μ L of a 2 mM solution of T-VPI ($2.5 \cdot 10^{-7}$ mol) in D₂O, 50 μ L of a 5 mM solution of CB[7] ($2.5 \cdot 10^{-7}$ mol) in D₂O, 25 μ L of a 200 mM solution of AgNO₃ in D₂O ($5 \cdot 10^{-6}$ mol) and 300 μ L of D₂O. ¹H NMR of CB[7]·T-VPI·Ag⁺ (500 MHz, D₂O, 298 K, 0.5 mM) δ 9.35 (br s, 2H, **H2**), 8.89 (br s, 4H, overlapped signals of **H3** and **H4**), 8.80 (br s, 2H, **H5**), 7.95 (br m, 4H, overlapped signals of **H7** and **H8** or **H9**), 7.52 (br s, 6H, overlapped signals of **H6**, **Hy** and **H8** or **H9**), 7.34 (br s, 2H, **Hx**), 5.71 (d, $J = 15.2$ Hz, 14H, CB[7]), 5.52 (br s, 14H, CB[7]), 4.23 (d, $J = 15.4$ Hz, 14H, CB[7]), 2.37 (br s, 3H, **H1**), 2.22 (acetone, ref). Figure S54.

2:1:1 complex: A 0.5 mM solution of CB[7]₂·T-VPI·Ag⁺ was prepared by addition of 125 μ L of a 2 mM solution of T-VPI ($2.5 \cdot 10^{-7}$ mol) in D₂O, 100 μ L of a 5 mM solution of CB[7] ($5 \cdot 10^{-7}$ mol) in D₂O, 25 μ L of a 200 mM solution of AgNO₃ in D₂O ($5 \cdot 10^{-6}$ mol) and 250 μ L of D₂O. ¹H NMR (500 MHz, D₂O) δ 9.28 (d, $J = 6.8$ Hz, 2H, **H2**), 9.07 (d, $J = 6.9$ Hz, 2H, **H4**), 9.04 (d, $J = 6.7$ Hz, 2H, **H3**), 8.49 (d, $J = 6.9$ Hz, 2H, **H5**), 7.99 (app t, $J = 8.1$ Hz, 2H, **H8-H8'** or **H9-H9'**), 7.70 (d, $J = 8.5$ Hz, 2H, **H7**), 7.61–7.52 (m, 2H, **H8-H8'** or **H9-H9'**), 6.98 (two d, $J = 8.5$ Hz, 4H, overlapped signals of **H6** and **Hy**), 6.65 (d, $J = 8.1$ Hz, 2H, **Hx**), 5.83 (d, $J = 15.5$ Hz, 7H, CB[7]), 5.79 (d, $J = 15.5$ Hz, 7H, CB[7]), 5.72 (d, $J = 15.5$ Hz, 14H, CB[7]), 5.52 (d, $J = 17.8$ Hz, 28H, CB[7]), 4.29–4.16 (m, 28H, CB[7]), 2.22 (acetone, ref), 2.01 (br s, 3H, **H1**). Figure S57.

Acknowledgements

CNRS and Aix Marseille Université are acknowledged for continuous support. This work received support from the French government under the France 2030 investment plan, as part of the Initiative d'Excellence d'Aix-Marseille Université - A*MIDEX.^a (AMX-20-IET-015). Mrs Virginie Heran (Aix-Marseille University, CNRS, iSm2, Marseille, France) is gratefully acknowledged for assistance regarding ITC measurements.

Conflict of Interests

The authors declare no conflict of interest.

Data Availability Statement

The data that support the findings of this study are available in the supplementary material of this article.

Keywords: cucurbituril · heterocycles · host:guest chemistry · macrocycles · viologens

- [1] a) P. L. Anelli, N. Spencer, J. F. Stoddart, *J. Am. Chem. Soc.* **1991**, *113*, 5131–5133; b) R. A. Bissell, E. Cordova, A. E. Kaifer, J. F. Stoddart, *Nature* **1994**, *369*, 133–137.
[2] a) S. Silvi, M. Venturi, A. Credi, *J. Mater. Chem.* **2009**, *19*, 2279–2294; b) A. Rescifina, C. Zagni, D. Iannazzo, P. Merino, *Curr. Org. Chem.* **2009**, *13*, 448–481; c) J. D. Crowley, S. M. Goldup, A.-L. Lee, D. A. Leigh, R. T. McBurney, *Chem. Soc. Rev.* **2009**, *38*, 1530–1541.

- [3] a) J. Berná, M. Alajarin, C. Marín-Rodríguez, C. Franco-Pujante, *Chem. Sci.* **2012**, *3*, 2314–2320; b) P. Langer, L. Yang, C. R. Pfeiffer, W. Lewis, N. R. Champness, *Dalton Trans.* **2019**, *48*, 58–64.
[4] M. Douarre, V. Martí-Centelles, C. Rossy, I. Pianet, N. D. McClenaghan, *Eur. J. Org. Chem.* **2020**, 5820–5827.
[5] J. O. Jeppesen, S. Nygaard, S. A. Vignon, J. F. Stoddart, *Eur. J. Org. Chem.* **2005**, 2005, 196–220.
[6] a) S. Garaudée, S. Silvi, M. Venturi, A. Credi, A. H. Flood, J. F. Stoddart, *ChemPhysChem* **2005**, *6*, 2145–2152; b) F. Coutrot, E. Busseron, *Chem. Eur. J.* **2008**, *14*, 4784–4787; c) N. Le Poul, B. Colasson, *ChemElectroChem* **2015**, *2*, 475–496; d) G. Ragazzon, A. Credi, B. Colasson, *Chem. Eur. J.* **2017**, *23*, 2149–2156.
[7] a) V. Aucagne, J. Berná, J. D. Crowley, S. M. Goldup, K. D. Hänni, D. A. Leigh, P. J. Lusby, V. E. Ronaldson, A. M. Z. Slawin, A. Viterisi, D. B. Walker, *J. Am. Chem. Soc.* **2007**, *129*, 11950–11963; b) N.-C. Chen, C.-C. Lai, Y.-H. Liu, S.-M. Peng, S.-H. Chiu, *Chem. Eur. J.* **2008**, *14*, 2904–2908; c) A. Coskun, D. C. Friedman, H. Li, K. Patel, H. A. Khatib, J. F. Stoddart, *J. Am. Chem. Soc.* **2009**, *131*, 2493–2495; d) C. Romuald, E. Busseron, F. Coutrot, *J. Org. Chem.* **2010**, *75*, 6516–6531; e) K. Zhu, V. N. Vukotic, S. J. Loeb, *Chem. Asian J.* **2016**, *11*, 3258–3266; f) P. Waeles, K. Fournel-Marotte, F. Coutrot, *Chem. Eur. J.* **2017**, *23*, 11529–11539; g) S. J. Vella, S. J. Loeb, *Beilstein J. Org. Chem.* **2018**, *14*, 1908–1916; h) A. Ghosh, I. Paul, M. Adlung, C. Wickleder, M. Schmittel, *Org. Lett.* **2018**, *20*, 1046–1049.
[8] a) V. A. Freeman, W. L. Mock, N. Y. Shih, *J. Am. Chem. Soc.* **1981**, *103*, 7367–7368; b) L. Isaacs, *Chem. Commun.* **2009**, 619–629.
[9] J. Kim, I.-S. Jung, S.-Y. Kim, E. Lee, J.-K. Kang, S. Sakamoto, K. Yamaguchi, K. Kim, *J. Am. Chem. Soc.* **2000**, *122*, 540–541.
[10] a) J. W. Lee, S. Samal, N. Selvapalam, H.-J. Kim, K. Kim, *Acc. Chem. Res.* **2003**, *36*, 621–630; b) J. Lagona, P. Mukhopadhyay, S. Chakrabarti, L. Isaacs, *Angew. Chem. Int. Ed.* **2005**, *44*, 4844–4870; *Angew. Chem.* **2005**, *117*, 4922–4949; c) M. V. Rekharsky, T. Mori, C. Yang, Y. H. Ko, N. Selvapalam, H. Kim, D. Sobransingh, A. E. Kaifer, S. Liu, L. Isaacs, W. Chen, S. Moghaddam, M. K. Gilson, K. Kim, Y. Inoue, *Proc. Natl. Acad. Sci. USA* **2007**, *104*, 20737–20742; d) E. Masson, X. Ling, R. Joseph, L. Kyremeh-Mensah, X. Lu, *RSC Adv.* **2012**, *2*, 1213–1247; e) S. J. Barrow, S. Kasper, M. J. Rowland, J. del Barrio, O. A. Scherman, *Chem. Rev.* **2015**, *115*, 12320–12406; f) K. I. Assaf, W. M. Nau, *Chem. Soc. Rev.* **2015**, *44*, 394–418; g) L. Mikulu, R. Michalicova, V. Iglesias, M. A. Yawer, A. E. Kaifer, P. Lubal, V. Sindelar, *Chem. Eur. J.* **2017**, *23*, 2350–2355; h) A. Palma, O. A. Artelsmaier, G. Wu, X. Lu, S. J. Barrow, N. Uddin, E. Rosta, E. Masson, O. A. Scherman, *Angew. Chem. Int. Ed.* **2017**, *56*, 15688–15692; *Angew. Chem.* **2017**, *129*, 15894–15898; i) E. Pazos, P. Novo, C. Peinador, A. E. Kaifer, M. D. García, *Angew. Chem. Int. Ed.* **2019**, *58*, 403–416; *Angew. Chem.* **2019**, *131*, 409–422; j) X. Yang, R. Wang, A. Kermagoret, D. Bardelang, *Angew. Chem. Int. Ed.* **2020**, *59*, 21280–21292; *Angew. Chem.* **2020**, *132*, 21464–21476; k) A. Hennig, W. M. Nau, *Monogr. Supramol. Chem.* **2020**, *28*, 121–149; l) C. Li, A.-D. Manick, Y. Zhao, F. Liu, B. Chatelet, R. Rosas, D. Siri, D. Gignes, V. Monnier, L. Charles, J. Broggi, S. Liu, A. Martinez, A. Kermagoret, D. Bardelang, *Chem. Eur. J.* **2022**, e202201656.
[11] a) X. Ling, E. L. Samuel, D. L. Patchell, E. Masson, *Org. Lett.* **2010**, *12*, 2730–2733; b) X. Ling, E. Masson, *Org. Lett.* **2012**, *14*, 4866–4869; c) L. Isaacs, *Acc. Chem. Res.* **2014**, *47*, 2052–2062; d) E. Y. Chernikova, D. V. Berdnikova, Y. V. Fedorov, O. A. Fedorova, F. Maurel, G. Jonusauskas, *Phys. Chem. Chem. Phys.* **2017**, *19*, 25834–25839; e) L. Zhu, M. Zhu, Y. Zhao, *ChemPlusChem* **2017**, *82*, 30–41; f) A. Zubillaga, P. Ferreira, A. J. Parola, S. Gago, N. Basilio, *Chem. Commun.* **2018**, *54*, 2743–2746; g) A. Seco, A. M. Diniz, J. Sarrato, H. Mourão, H. Cruz, A. J. Parola, N. Basilio, *Pure Appl. Chem.* **2020**, *92*, 301–313; h) J.-X. Liu, K. Chen, C. Redshaw, *Chem. Soc. Rev.* **2023**, 10.1039/D1032CS00785A.
[12] a) F. J. McInnes, N. G. Anthony, A. R. Kennedy, N. J. Wheate, *Org. Biomol. Chem.* **2010**, *8*, 765–773; b) V. Kolman, M. S. A. Khan, M. Babinsky, R. Marek, V. Sindelar, *Org. Lett.* **2011**, *13*, 6148–6151; c) L. Zhu, H. Yan, X.-J. Wang, Y. Zhao, *J. Org. Chem.* **2012**, *77*, 10168–10175; d) H. Zhang, L. Liu, C. Gao, R. Sun, Q. Wang, *Dyes Pigm.* **2012**, *94*, 266–270; e) M. Freitag, L. Gundlach, P. Piotrowiak, E. Galoppini, *J. Am. Chem. Soc.* **2012**, *134*, 3358–3366; f) X.-L. Ni, J.-M. Yi, S. Song, Y.-Q. Zhang, S.-F. Xue, Q.-J. Zhu, Z. Tao, *Tetrahedron* **2013**, *69*, 6219–6222; g) M. Baroncini, C. Gao, V. Carboni, A. Credi, E. Previtiera, M. Semeraro, M. Venturi, S. Silvi, *Chem. Eur. J.* **2014**, *20*, 10737–10744; h) N. Basilio, V. Petrov, F. Pina, *ChemPlusChem* **2015**, *80*, 1779–1785; i) E. Y. Chernikova, S. V. Tkachenko, O. A. Fedorova, A. S. Peregodov, I. A. Godovikov, N. E. Shepel, S. Minkovska, A. Kurutos, N. Gadjev, T. G. Deligeorgiev, Y. V. Fedorov, *Dyes Pigm.* **2016**, *131*, 206–214; j) W. Wu, S. Song, X. Cui, T. Sun, J.-X. Zhang, X.-L. Ni, *Chin. Chem. Lett.* **2018**, *29*, 95–98; k) X. Zhang, X. Shi, S. Su, G.

- Zhou, X.-L. Ni, *Dyes Pigm.* **2020**, *172*, 107785; l) F. Liu, H. Karoui, A. Rockenbauer, S. Liu, O. Ouari, D. Bardelang, *Molecules* **2020**, *25*, 776; m) R.-L. Lin, R. Li, H. Shi, K. Zhang, D. Meng, W.-Q. Sun, K. Chen, J.-X. Liu, *J. Org. Chem.* **2020**, *85*, 3568–3575.
- [13] V. Sindelar, S. Silvi, A. E. Kaifer, *Chem. Commun.* **2006**, 2185–2187.
- [14] H. Shi, K. Zhang, R.-L. Lin, W.-Q. Sun, X.-F. Chu, X.-H. Liu, J.-X. Liu, *Asian J. Org. Chem.* **2019**, *8*, 339–343.
- [15] Y. Gong, H. Chen, X. Ma, H. Tian, *ChemPhysChem* **2016**, *17*, 1934–1938.
- [16] A. Seco, S. Yu, A. Tron, N. D. McClenaghan, F. Pina, A. Jorge Parola, N. Basilio, *Chem. Eur. J.* **2021**, *27*, 16512–16522.
- [17] Q. Cheng, H. Yin, R. Rosas, D. Gigmes, O. Ouari, R. Wang, A. Kermagoret, D. Bardelang, *Chem. Commun.* **2018**, *54*, 13825–13828.
- [18] H. Yin, Q. Cheng, R. Rosas, S. Viel, V. Monnier, L. Charles, D. Siri, D. Gigmes, O. Ouari, R. Wang, A. Kermagoret, D. Bardelang, *Chem. Eur. J.* **2019**, *25*, 12552–12559.
- [19] F. Liu, S. Chowdhury, R. Rosas, V. Monnier, L. Charles, H. Karoui, D. Gigmes, O. Ouari, F. Chevallier, C. Bucher, A. Kermagoret, S. Liu, D. Bardelang, *Org. Lett.* **2021**, *23*, 5283–5287.
- [20] H. Yin, R. Rosas, D. Gigmes, O. Ouari, R. Wang, A. Kermagoret, D. Bardelang, *Org. Lett.* **2018**, *20*, 3187–3191.
- [21] Additional experimental data supporting formation of a VPI–N dimer will be reported in a subsequent paper.
- [22] X. Yang, Q. Cheng, V. Monnier, L. Charles, H. Karoui, O. Ouari, D. Gigmes, R. Wang, A. Kermagoret, D. Bardelang, *Angew. Chem. Int. Ed.* **2021**, *60*, 6617–6623; *Angew. Chem.* **2021**, *133*, 6691–6697.
- [23] L. Zhang, V. Marcos, D. A. Leigh, *Proc. Natl. Acad. Sci. USA* **2018**, *115*, 9397–9404.
- [24] G. A. Vincil, A. R. Urbach, *Supramol. Chem.* **2008**, *20*, 681–687.
- [25] F. Biedermann, V. D. Uzunova, O. A. Scherman, W. M. Nau, A. De Simone, *J. Am. Chem. Soc.* **2012**, *134*, 15318–15323.
- [26] F. Biedermann, M. Vendruscolo, O. A. Scherman, A. De Simone, W. M. Nau, *J. Am. Chem. Soc.* **2013**, *135*, 14879–14888.
- [27] P. Setny, R. Baron, J. A. McCammon, *J. Chem. Theory Comput.* **2010**, *6*, 2866–2871.
- [28] F. Benyettou, K. Nchimi-Nono, M. Jouiad, Y. Lalatonne, I. Milosevic, L. Motte, J.-C. Olsen, N. I. Saleh, A. Trabolssi, *Chem. Eur. J.* **2015**, *21*, 4607–4613.
- [29] D. Bardelang, K. A. Udachin, D. M. Leek, J. C. Margeson, G. Chan, C. I. Ratcliffe, J. A. Ripmeester, *Cryst. Growth Des.* **2011**, *11*, 5598–5614.

Manuscript received: February 27, 2023

Accepted manuscript online: April 17, 2023

Version of record online: April 27, 2023